# Structure of Aggregated Gold Colloids

P. Dimon, S. K. Sinha, D. A. Weitz, C. R. Safinya, G. S. Smith,[a] W. A. Varady, and H. M. Lindsay
*Exxon Research and Engineering Company, Annandale, New Jersey 08801*
(Received 19 February 1986)

We report a high-resolution, small-angle x-ray study of aggregated gold colloids over the range 0.0003 to 0.08 Å$^{-1}$. We are able to fit our data with a simple model that correctly accounts for nonfractal short-range order with a crossover to long-range fractal correlations. This provides new information on the structure of real aggregates, and new insight into the aggregation processes which lead to their formation.

PACS numbers: 64.60.Cn, 05.40.+j, 61.10.Lx, 82.70.Dd

What is the structure of an aggregate? Several years ago, Witten and Sander[1] showed that aggregates can be statistically scale-invariant objects, physical realizations of mathematical fractals[2] which appear the same on all length scales. This property manifests itself in a power-law dependence of the density-density correlation function, i.e., $G(r) \sim r^{D-d}$, where $d$ is the spatial dimension and $D$ is the fractal dimension ($D < d$). These results have been elucidated by computer simulations of several different models including the diffusion-limited aggregation (DLA) model,[1,3] the diffusion-limited cluster aggregation (DLCA) model,[4] and the reaction-limited cluster aggregation (RLCA) model.[5] Experimentally, aggregates of gold colloids[6-8] and silica particles[9-11] have been studied with light, neutron, and low-resolution x-ray scattering. The emphasis of most studies to date has been the fractal nature of the aggregates. However, in reality, objects can be scale invariant only over a limited range, and an understanding of the bounds of the fractal regime is crucial in the development of a complete picture, not only of aggregates, but of fractal objects in general. In particular, as we shall see, the short-range order, or correlations of the nearest neighbors, cannot be treated as fractal. However, these correlations play an important role in determining the physical properties of the ultimate structure and, in addition, offer important clues about the interparticle interactions involved in the aggregation process itself. In this paper, we report the results of a high-resolution x-ray scattering experiment using colloidal gold aggregates, and present data that extend over both the conventional light and small-angle x-ray and neutron scattering regimes. This study, with momentum transfers (length scales) continuously ranging from 0.0003 Å$^{-1}$ ($\sim$3000 Å) to 0.08 Å$^{-1}$ ($\sim$10 Å) and on samples comprising over $10^6$ clusters, provides the most definitive probe of the fractal structure of aggregates. The excellent statistics and the wide range of these data allow us to probe both the fractal regime of the aggregate structure and the crossover regime where the nonfractal short-range order dominates. A simple model is developed to account quantitatively for these data, and the short-range correlations thus determined are related to the kinetic growth processes that form the aggregate.

Three samples of aggregated gold colloids comprised of $\sim$75-Å-radius, polycrystalline gold balls[6] were studied. The colloids were aggregated by reduction of the charge on the surface of the particles causing them to stick upon diffusion-induced collision. In one case, the charge was completely removed so that the diffusion of the clusters was the rate-limiting process, resulting in DLCA. In the second case, the charge was only slightly reduced, so that the actual chemical bond formation was the rate-limiting process, resulting in RLCA. The scattering was done from clusters large enough to precipitate, thus increasing the volume fraction of gold from its initial value of $10^{-6}$ to roughly $10^{-3}$. The precipitate solution was placed between two 0.127-mm Kapton sheets. The experiment was done on beamline VI-2 at the Stanford Synchrotron Radiation Laboratory with 1.54-Å x rays. We used a double-bounce Si(111) monochromator and a triple-bounce Si(111) analyzer in the nondispersive configuration to obtain a sharp Gaussian in-plane resolution function with rms width $6\times10^{-5}$ Å$^{-1}$. The out-of-plane resolution function was determined by a set of extremely narrow slits, yielding a Gaussian out-of-plane resolution function of rms width $3.4\times10^{-4}$ Å$^{-1}$. The sharpness of the resolution function enabled us to reach momentum transfers of 0.0003 Å$^{-1}$ before we were swamped by the main beam.

Figure 1 shows the background-subtracted data for the RLCA sample, corrected for the transmission factor. At small $Q$, the data clearly show power-law behavior reflecting the long-range fractal correlations, while at large $Q$, the behavior is dominated by the form factor of the individual gold balls comprising the aggregate. However, a model which includes only a fractal $S(Q)$ modified by the form factor of a single gold ball, as was used to account for previous neutron- and light-scattering data from gold aggregates,[8] cannot describe the present, more extensive data. To account for these data we must include short-range nonfractal correlations. Physically, we expect that $G(r) \sim r^{D-3}$ should only be valid for $r$ greater than a few ball diam-

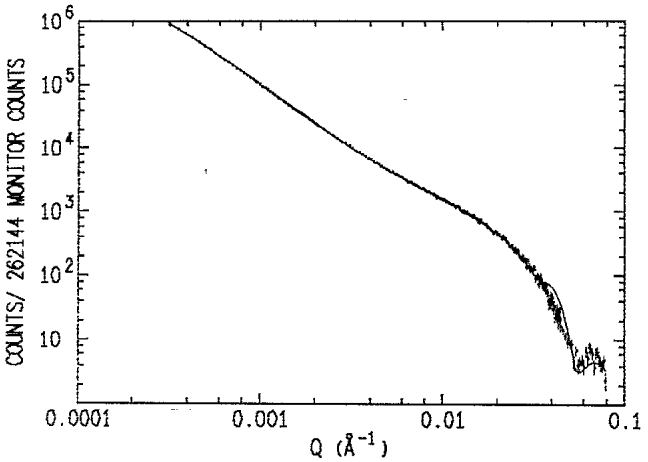


FIG. 1. Background-subtracted data of RLCA sample. The solid line is a fit by our model (see text). The range in $Q$ probed corresponds to length scales of $\sim 3000$ Å (0.0003 Å$^{-1}$) to $\sim 10$ Å (0.08 Å$^{-1}$). The background level was $\sim 1\%$ of the total signal.

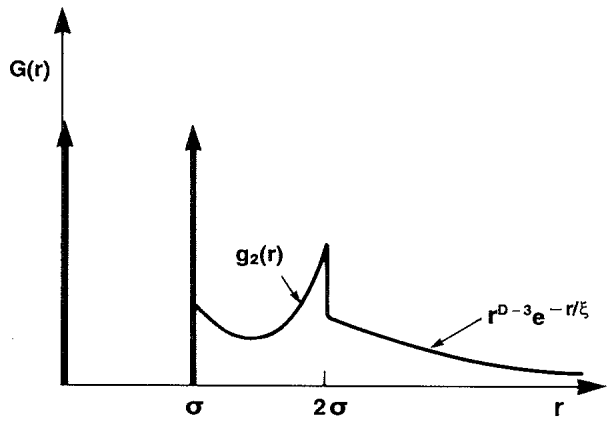


FIG. 2. Correlation function $G(r)$ used in our model [see Eq. (1)].

eters. For shorter distances, we can model the aggregate as being comprised of hard spheres in close contact. If we assume an isotropic aggregate, the correlation function can be expressed in the following form (see Fig. 2):

$$G(r)=\begin{cases}\delta(\mathbf{r})+(z_1/4\pi\sigma^2)\delta(r-\sigma) & (r\leq\sigma),\\ z_2 g_2(r) & (\sigma<r<2\sigma),\\ A_f B r^{D-3}e^{-r/\xi} & (r>2\sigma).\end{cases} \tag{1}$$

The δ function at the origin is due to self-correlations. The δ function at $r=\sigma$, where $\sigma$ is a ball diameter, reflects the presence of nearest neighbors in hard contact with the ball at the origin. Thus, $z_1$ is the coordination number of this first shell. The second line of Eq. (1) represents the second shell, whose presence was inferred from computer simulations of both random-packed hard spheres[12] and DLCA aggregates.[13] $g_2(r)$ is a second-order polynomial fit to the hard-sphere simulation data with $4\pi\int_\sigma^{2\sigma} g_2(r)r^2dr=1$ so that $z_2$ is the second-shell coordination number. We found that including this term made the fits somewhat better but was not essential. The last line of Eq. (1) describes the crossover to long-range fractal correlations. (A correlation length $\xi$ has been included to account for overlap among clusters,[10] but because of their size, it was found to be effectively infinite.) $B$ is a constant defined so that $G(r)$ is continuous at $r=2\sigma$ when $A_f=1$, i.e., $z_2g_2(2\sigma)=B(2\sigma)^{D-3}e^{-2\sigma/\xi}$. $A_f$ therefore measures the amplitude of the fractal term relative to the second-shell term at $r=2\sigma$. There are thus four adjustable parameters in the model: $D$, $z_1$, $z_2$, and $A_f$.

The structure factor for the aggregate is then given by the Fourier transform of $G(r)$:

$$S_A(Q)=1+z_1\sin Q\sigma/Q\sigma+(4\pi z_2/Q)\int_\sigma^{2\sigma} rg_2(r)\sin Qr\,dr+(4\pi A_fB/Q)\int_{2\sigma}^{\infty} r^{D-2}e^{-r/\xi}\sin Qr\,dr. \tag{2}$$

The second integral in Eq. (2) can be expressed as an incomplete gamma function and evaluated numerically by series expansions. The actual measured intensity is given by

$$I(\mathbf{Q})=\int |f(Q'r_0)|^2 S_A(Q')R(\mathbf{Q}-\mathbf{Q}')d^3Q', \tag{3}$$

where $f(Qr_0)$ is the form factor of a gold ball of radius $r_0$ and $R(\mathbf{Q}-\mathbf{Q}')$ is the resolution function discussed earlier. For small-angle scattering geometry, we can take

$$R(\mathbf{Q}-\mathbf{Q}')\sim\exp[-(Q_x-Q_x')^2/2\sigma_x^2]\exp(-Q_z'^2/2\sigma_z^2)\delta(Q_y'),$$

where $Q_x$ and $Q_y$ are in the scattering plane, and the scan is done along $Q_x$. As stated earlier, $\sigma_x=6\times10^{-5}$ Å$^{-1}$ and $\sigma_z=3.4\times10^{-4}$ Å$^{-1}$. Proper inclusion of the resolution function is essential as it will always result in the fitted fractal dimension being slightly larger ($\sim 10\%$ in our experiments) than if it were measured directly from the data.

It is also necessary to consider the effects of polydispersity in the analysis. So far it has been assumed that the gold balls are uniform in size. If this were true, the first minimum in the form factor at $\sim 0.06$ Å$^{-1}$ would be identically zero resulting in a sharp dip where we see only a shallow one. In a polydisperse system we have

$$S(\mathbf{Q})=\frac{1}{N}\sum_i |f_i(\mathbf{Q})|^2+\frac{1}{N}\sum_{i\neq j} f_i(\mathbf{Q})f_j^*(\mathbf{Q})\exp[i\mathbf{Q}\cdot(\mathbf{r}_i-\mathbf{r}_j)],$$

or, replacing the sums by averages, we can substitute

$$|f(Qr_0)|^2 S_A(Q) \rightarrow \langle |f(Qr_0)|^2 \rangle + |\langle f(Qr_0) \rangle|^2 [S_A(Q) - 1]$$

in Eq. (3), where $\langle\ \rangle$ signifies an average over the distribution of ball sizes. If the distribution is Gaussian, then for any function $h(r_0)$,

$$\langle h(r_0) \rangle = \frac{1}{(2\pi)^{1/2}\delta_P} \int_0^\infty h(r_0) \exp[-(r_0 - \bar{r})^2/2\delta_P^2]\, dr_0,$$

where $\bar{r}$ is the mean radius, and $\delta_P$ is the rms width. The normalization constant is based on the assumption that the unphysical range $(-\infty, 0)$ contributes negligibly in the integral if $\delta_P$ is small compared with $\bar{r}$. We found empirically that $\bar{r} = 79$ Å and $\delta_P = 0.1r$ reproduced the position and size of the dip in the RLCA data. This is actually consistent with previous transmission-electron-microscopy measurements which found $\bar{r} \sim 75$ Å and rms deviations from 8% to 13%.[14] Different values for the polydispersity did not affect the fits greatly. Polydispersity will also smear the form of $S_A(Q)$ in Eq. (2), but these effects were investigated and found to be unimportant.

The result of the fitting of Eq. (3) to the RLCA data is shown in Fig. 1. We find that $D = 2.20$, a number somewhat higher than previous results.[7] This number is essentially model independent (not including resolution effects), being determined primarily by the data at small $Q$ where the statistics are superior and short-range effects are unimportant. The first-shell coordination number is $z_1 = 2.33$, which, considering this was a free parameter, is not unreasonable for such a tenuous object as an aggregate. (In his simulations of the DLA model, Meakin[3] found $z_1 = 2.25$.) Also, $z_2 = 3.95$, which is larger than $z_1$, as it should be. The parameter $A_f$ is 0.46, which is consistent with computer simulations of random packed hard spheres[12] and aggregates.[13] The small shoulder in the fit at $Q \sim 0.04$ Å$^{-1}$ arises from the $\delta$ function in $G(r)$ at $r = \sigma$ and probably reflects our imperfect knowledge of $G(r)$.

Our model is not as successful in accounting for the complete set of data for the DLCA sample, as shown in Fig. 3. At small $Q$, unlike the RLCA sample, the data had an upward turn which could not be explained by the present model. The origin of this will be discussed shortly. However, if we use only the data above 0.002 Å$^{-1}$, a good fit is obtained with our model. The value of $D = 1.73$ obtained for the fractal dimension agrees with previous measurements[6,7] and is consistent with the DLCA model in three dimensions.[4] Interestingly, we obtain $z_1 = 3.14$, which is substantially higher than the RLCA sample. The other fitted parameters were $z_2 = 4.86$ and $A_f = 0.43$. As a test, we also fitted the RLCA data only using the points with $Q > 0.002$ Å$^{-1}$ to see if it significantly affected the fit, but it did not. A second DLCA sample was studied with similar results to the first except that its transmission factor for x rays was 200 times greater. This should rule out any multiple-scattering effects in these experiments.

An important result obtained by the fitting of our model to the data is that the first-shell coordination number for the DLCA sample is larger than for the RLCA sample, even though an aggregate prepared by DLCA is less dense.[6] It is known that in DLCA the potential between balls consists solely of an attractive van der Waals interaction, while in RLCA there is a Coulombic repulsion.[7] Presumably, then, in the early stages of the aggregation process, it is more favorable for a ball to stick to several balls in DLCA ($z_1 > 2$), but to only one ball in RLCA ($z_1 \sim 2$). As the clusters get larger, however, these same properties in the potential will allow clusters formed by RLCA to interpenetrate more deeply, while in DLCA they will stick at the first contact, forming a less packed, more tenuous structure. These differences in first-shell coordination number can be expected to have large effects on the physical properties of the resultant aggregates, such as their conductivity and mechanical strength. Thus, our interpretation of these measurements provides insight into the early stages of the aggregation process and the effects of realistic interparticle potentials. Such interactions have not as yet been included

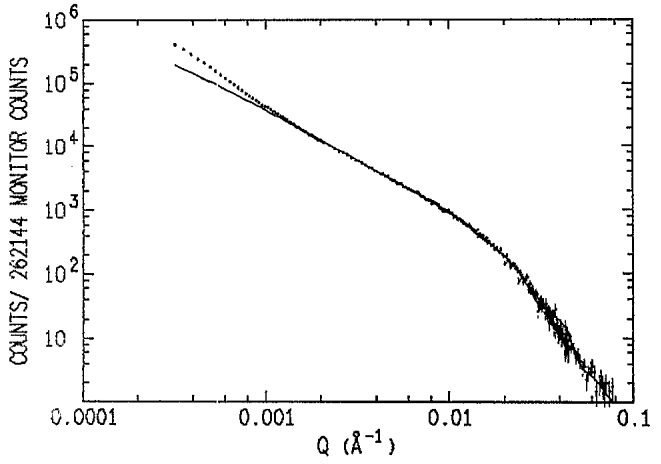


FIG. 3. Background-subtracted data of DLCA sample No. 1. The solid line is a fit to our model using only the data points above 0.002 Å$^{-1}$, but extended to smaller $Q$ to show how the slope in the data increases there. The effective length scales and background level are the same as in Fig. 1.

in any simulations.

Finally, we discuss the upward turn at small $Q$ in the DLCA data. We believe that this reflects a restructuring of the aggregates,[11,15] which results in an apparent increase in the power law of the scattering at small $Q$, for distances greater than $\sim 1000$ Å. While this implies that the density is decreasing less rapidly than at shorter length scales, we cannot confirm that this large scale structure is fractal. It is significant that we observe this effect only for the DLCA samples which have lower fractal dimensions and are thus more tenuous and presumably structurally weaker than the RLCA sample. Further confirmation of this behavior was obtained from light-scattering measurements covering the range $2.5\times10^{-4}$ Å$^{-1} \leq Q \leq 3\times10^{-3}$ Å$^{-1}$. Freshly prepared aggregates exhibited a clear fractal behavior with $D \sim 1.75$, while those that had been aged several days and subjected to shears similar to those of the x-ray samples showed an apparent fractal dimension of $D \sim 2.4$, which is roughly the same as the small-$Q$ slope in the x-ray data. Similar observations have been reported for DLCA silica aggregates.[11] We note, however, that the x-ray data show that at short length scales the original fractal structure is preserved, while the restructuring occurs primarily at larger length scales.

In conclusion, we have shown that a more physical model of an aggregate which includes the short-range order is capable of accurately describing our data. The aggregates we have studied are consistent with a fractal interpretation over the length scales we have probed. However, it is crucial to include the short-range order to interpret the scattering data correctly. In so doing, it is also possible to extract information about the effects of interparticle interactions on the aggregation process.

It is a pleasure to acknowledge discussions with T. Witten, J. Gethner, R. Pynn, R. Ball, M. Y. Lin, M. O. Robbins, and W. D. Dozier. One of us (G.S.S.) acknowledges support from National Science Foundation Grant No. DMR-8307157. We would also like to thank the staff of Stanford Synchrotron Radiation Laboratory for their kind assistance.

[a] Also at Department of Physics, University of Colorado, Boulder, CO 80309.

[1] T. A. Witten and L. M. Sander, Phys. Rev. Lett. **47**, 1400 (1981), and Phys. Rev. B **27**, 5686 (1983).

[2] B. B. Mandelbrot, *The Fractal Geometry of Nature* (Freeman, San Francisco, 1982).

[3] P. Meakin, Phys. Rev. A **27**, 604, 1495 (1983).

[4] P. Meakin, Phys. Rev. Lett. **51**, 1119 (1983); M. Kolb, R. Botet, and R. Jullien, Phys. Rev. Lett. **51**, 1123 (1983); R. Jullien, M. Kolb, and R. Botet, J. Phys. (Paris), Lett. **45**, L211 (1984).

[5] M. Kolb and R. Jullien, J. Phys. (Paris), Lett. **45**, L977 (1984).

[6] D. A. Weitz and M. Oliveria, Phys. Rev. Lett. **52**, 1433 (1984).

[7] D. A. Weitz, J. S. Huang, M. Y. Lin, and J. Sung, Phys. Rev. Lett. **54**, 1416 (1985).

[8] D. A. Weitz, M. Y. Lin, J. S. Huang, T. A. Witten, S. K. Sinha, J. S. Gethner, and R. C. Ball, in *Scaling Phenomena in Disordered Systems,* edited by R. Pynn and A. Skjeltorp (Plenum, New York, 1985), p. 171.

[9] D. W. Schaefer, J. E. Martin, P. Wiltzius, and D. S. Cannell, Phys. Rev. Lett. **52**, 2371 (1984).

[10] S. K. Sinha, T. Freltoft, and J. Kjems, in *Kinetics of Aggregation and Gelation,* edited by F. Family and D. P. Landau (North-Holland, Amsterdam, 1984), p. 87; T. Freltoft, J. K. Kjems, and S. K. Sinha, Phys. Rev. B **33**, 269 (1986).

[11] C. Aubert and D. S. Cannell, Phys. Rev. Lett. **56**, 738 (1986).

[12] C. H. Bennett, J. Appl. Phys. **43**, 2727 (1972).

[13] P. Meakin, private communication.

[14] J. Turkevich, P. C. Stevenson, and J. Hillier, Discuss. Faraday Soc. **11**, 55 (1951).

[15] Y. Kantor and T. A. Witten, J. Phys. (Paris), Lett. **45**, L675 (1984).